Functional indicators of response mechanisms to nitrogen deposition, ozone, and their interaction in two Mediterranean tree species

Lina Fusaro[1]*, Adriano Palma[1], Elisabetta Salvatori[1], Adriana Basile[2], Viviana Maresca[2], Elham Asadi Karam[3], Fausto Manes[1]

1 Sapienza University of Rome, Department of Environmental Biology, Rome, Italy, **2** University of Naples "Federico II", Biology Department, Naples, Italy, **3** Shahid Bahonar University of Kerman, Biology Department, Kerman, Iran

* lina.fusaro@uniroma1.it

Abstract

The effects of nitrogen (N) deposition, tropospheric ozone (O_3) and their interaction were investigated in two Mediterranean tree species, *Fraxinus ornus* L. (deciduous) and *Quercus ilex* L. (evergreen), having different leaf habits and resource use strategies. An experiment was conducted under controlled condition to analyse how nitrogen deposition affects the ecophysiological and biochemical traits, and to explore how the nitrogen-induced changes influence the response to O_3. For both factors we selected realistic exposures (20 kg N ha^{-1} yr^{-1} and 80 ppb h for nitrogen and O_3, respectively), in order to elucidate the mechanisms implemented by the plants. Nitrogen addition resulted in higher nitrogen concentration at the leaf level in *F. ornus*, whereas a slight increase was detected in *Q. ilex*. Nitrogen enhanced the maximum rate of assimilation and ribulose 1,5-bisphosphate regeneration in both species, whereas it influenced the light harvesting complex only in the deciduous *F. ornus* that was also affected by O_3 (reduced assimilation rate and accelerated senescence-related processes). Conversely, *Q. ilex* developed an avoidance mechanism to cope with O_3, confirming a substantial O_3 tolerance of this species. Nitrogen seemed to ameliorate the harmful effects of O_3 in *F. ornus*: the hypothesized mechanism of action involved the production of nitrogen oxide as the first antioxidant barrier, followed by enzymatic antioxidant response. In *Q. ilex*, the interaction was not detected on gas exchange and photosystem functionality; however, in this species, nitrogen might stimulate an alternative antioxidant response such as the emission of volatile organic compounds. Antioxidant enzyme activity was lower in plants treated with both O_3 and nitrogen even though reactive oxygen species production did not differ between the treatments.

Competing interests: The authors have declared that no competing interests exist.

Introduction

Mediterranean forests are subjected to challenging environmental conditions in the current global change context, since many stressors, individually or in combination, affect plant functionality simultaneously or successively over time [1]. Of more recent concern are the combined effects of ozone (O_3) and nitrogen (N) on vegetation [2]. Monitoring activities in European countries have indicated that studies on O_3 exposure effects are essential in Mediterranean regions [3], where the concurrence of high temperature and radiation promote the photo-stationary cycle toward high O_3 concentration during the late spring and summer seasons [4].

O_3 impacts forests by increasing the oxidation load, thereby triggering the production of reactive oxygen species (ROS) that lead to alterations of functional processes at different levels [5,6]. The production of ROS activates the detoxifying barrier in the apoplast and enzymatic activity at the symplastic level that have high metabolic cost [7,8], and the capacity to increase antioxidant defences is recognized as a key factor in determining O_3 tolerance [9–12].

Leaf gas exchange is also affected by O_3 through a direct impact on stomatal guard cell functionality [13,14] or stomatal number [15], as well as owing to a decrease in the photochemical and carboxylation efficiency [15–18]. Leaf structural traits such as leaf mass area (LMA), in addition to leaf nitrogen and carbon concentrations, have been found to reveal ozone sensitivity and tolerance in different species [19,20], where species with low LMA and high leaf nitrogen concentration show higher O_3 sensitivity [11,21]. Further, O_3 can adversely influence these functional traits, accelerating leaf senescence processes [22–24].

Nitrogen deposition represents an additional threat for Mediterranean forests adapted to low nitrogen availability [25]. During the last decades many studies have evaluated the effects of nitrogen on plant biodiversity and carbon balance or assimilation capacity [26–30], but many of them have been conducted on pastures [31], boreal and temperate forest species [26], or in Chaparral species [32,33]. The implications concerning Mediterranean forests are still scarce [34], and knowledge regarding the response of the large plethora of functional traits to increasing nitrogen deposition for forest species is lacking [15,35,36]. In Italy, the average nitrogen throughfall, in terms of NO_3NH_4, measured using the network of permanent monitoring stations, ranges between 4 and 29 kg N ha^{-1} yr^{-1} [37], and the critical loads indicated for Mediterranean forest ecosystems that fall within the range of 10 to 15 kg N ha^{-1} yr^{-1} have low reliability owing to the lack of experimental evidence [26].

Previous studies have shown that higher nitrogen availability can increase stomatal conductance [38,39], entailing a potential harmful increase in O_3 uptake. However the effects of nitrogen on hydraulic architecture and stomatal conductance are still contradictory [40]. Higher leaf nitrogen contents can result in photosynthetic enhancements owing to the key role that nitrogen has in Calvin cycle and proteins [41], or by the increase of leaf area. Recent studies on the interaction between O_3 and nitrogen deposition in deciduous species have highlighted that O_3 reduced the nitrogen availability for photosynthesis in *Fagus crenata* [42]; further, the positive effect on root development owing to nitrogen, is lost at higher O_3 levels in *Quercus robur* L. [43]. An antagonistic effect was detected on root starch concentrations, where higher nitrogen levels alleviated the negative impact of ozone [39]. Recent findings suggested that the interactions between O_3 and nitrogen depend on the concentration of these two factors and can change throughout the growing season [2]. Therefore, experiments under controlled conditions are required to better elucidate the mechanisms underlying the influence of nitrogen on the key functional traits that are involved in pollutant uptake or antioxidant defence mechanisms [2].

Moreover, species can remarkably differ in nitrogen absorption depending on the successional stage and resource allocation strategy [44,45]. Deciduous species tend to allocate

nitrogen to ribulose-1, 5-bisphosphate carboxylase/oxygenase (Rubisco), or to light-harvesting components in order to enhance the photosynthetic capacity; in contrast, in evergreen species, nitrogen is preferentially allocated to the cell walls, leading to an increase in the persistence of leaves [46,47], as well as toughness and chemical defence [48].

In this framework, we performed an experiment under controlled conditions to investigate how *Fraxinus ornus* L. and *Quercus ilex* L. react to nitrogen addition, and how nitrogen availability can influence the response mechanisms to O_3. For both factors, we selected realistic exposures (20 kg N ha^{-1} yr^{-1} and 80 ppb h for N and O_3, respectively), since an acute exposure could hinder the elucidation of mechanisms implemented by the plants [2]. We focused on these two species that typically co-occur in Mediterranean forests [49], and have different functional traits and successional positions. *F. ornus* is typical of early successional stages, with a rapid growth strategy, whereas *Q. ilex* belongs to the mature stage of a succession with a slow growth strategy and a conservative patterns of nutrient use [50]. Moreover, previous studies have suggested that *F. ornus* is moderately sensitive to O_3 [51], whereas *Q. ilex* was considered to be tolerant to this pollutant [11,15,52]; however, to the best of our knowledge, these two species have not yet been compared directly.

Owing to leaf habit and more flexible patterns of nitrogen uptake in *F. ornus* than in *Q. ilex* [53], we hypothesized that *F. ornus* uptakes a large amount of nitrogen and allocates higher fraction to photosynthetic tissues; in contrast, in *Q. ilex*, we expected that nitrogen would be allocated to non-photosynthetic compounds. Since both the hypothesized species-specific responses to nitrogen are related to O_3 tolerance, nitrogen addition could lead to mitigation of O_3 detrimental effects on functional traits. The present study provides new data on *F. ornus* and *Q. ilex* that would be useful to improve the risk assessment for Mediterranean forests subjected to nitrogen deposition and ozone. Furthermore, understanding the mechanisms underlying functional trait shifts under multistress environments could facilitate the forecasting of forests' responses to global change and addressing biodiversity conservation in the future.

Materials and methods

Growth conditions

Two-year-old seedlings of *F. ornus* and *Q. ilex*, obtained from the nursery of Aurunci Regional Park (Central Italy), were transported to the experimental garden of the Department of Environmental Biology, Sapienza University of Rome on 18 May 2016. Plants were transferred to 7L pots along with their clods and the remaining pot volume was filled with a mixture of sand, turf, and perlite. The experiment was conducted in a 'walk-in' chamber facility, consisting of two closed chambers (2.5 m × 3.9 m × 3 m h): one was used as control and one for O_3 fumigation [54]. Air temperature was maintained at 27.9 ± 1.8°C during the day and at 22.7 ± 0.9°C at night. The relative humidity was 61 ± 6.1%.

In each chamber, a photosynthetic active radiation of approximately 700 µmol m^{-2} s^{-1} was provided for 12 h per day by using 6 metal halide lamps (1000 W; Philips HPI-T). The microclimatic conditions were monitored at 5-min intervals and did not differ significantly between the chambers. In each chamber, plants were randomly relocated daily to reduce possible position effects. During the entire experimental period, all plants were watered in order to maintain soil close to field capacity and avoid water stress.

Experimental design

After the plants were acclimated for 30 days to the chamber environmental conditions, 20 plants per species were randomly divided into four experimental sets (C, N, O_3, and O_3N). Ten plants per species were assigned to the control chamber and thus randomly divided as

follows: five plants to the control experimental set (C), and five plants to nitrogen addition experimental set (N). Ten plants per species were assigned to the fumigated chamber and thus randomly divided as follows: five plants to the O_3 treatment (O_3), and five plants to the interaction experimental set, treated with both N and O_3 (O_3N).

The fertilizer was divided into 7 aliquots and applied throughout the experimental period as an aqueous solution. For this, 100 mL of deionised water was weekly added to each pot with different doses of ammonium nitrate (NH_4NO_3): 0 mg for C plants and 0.031 mg for N treatment. The final nitrogen dose was equal to 20 kg N ha^{-1} yr^{-1} based on the soil surface area. The ozone fumigation was started after five nitrogen additions, when the cumulative dose was roughly equivalent to 14 kg N ha^{-1} yr^{-1}, which falls in the upper limit of the threshold load currently indicated as critical for Mediterranean vegetation. The acclimation to nitrogen addition phase and fumigation period lasted 30 days and 10 days, respectively.

During the fumigation period, the C and N experimental sets were kept in the control chamber under filtered air (O_3 = 0 to maximal 5.8 ppb). The O_3 and O_3N sets were placed in the fumigation chamber and exposed for 10 consecutive days to a mean hourly O_3 concentration of 87.00 ± 0.5 ppb for 5 h per day simulating a concentration found in the Mediterranean rural area during the summer period [55,56]. The cumulative exposure was 2585.47 ppb h, expressed as AOT40, calculated by summing up all of the exceedances of the hourly O_3 concentration above 40 ppb during the daylight hours [56]. O_3 was generated in the fumigation chamber by flowing pure oxygen on a UV light source (Helios Italquartz, Milan, Italy), and then added to the chamber air inlet via a Teflon tube. The O_3 concentration at plant height was continuously monitored using a photometric O_3 detector (Model 205;, 2B Technologies, Boulder, CO, USA).

Leaf gas exchange and chlorophyll (Chl) *a* fluorescence were measured every three days, particularly on the first, fourth, seventh and tenth day of fumigation (DOF). Immediately after the end of fumigation, leaves for biochemical analysis (antioxidant activity) and structural measurements (nitrogen and carbon concentration, leaf mass area) were sampled; P_N/C_i curves were performed within two days. Further details about the measurements are provided below.

Gas exchange measurements

Steady state measurements of gas exchange were performed using a portable infrared gas analyser (CIRAS-2; PP-System International, Amesbury, MA). The net photosynthesis (P_N, $\mu mol CO_2$ m^{-2} s^{-1}), leaf transpiration (E, $mmol H_2O$ m^{-2} s^{-1}), stomatal conductance (gs, $mmol H_2O$ m^{-2} s^{-1}) and sub-stomatal CO_2 concentration (C_i, ppm) were simultaneously measured. The instantaneous water use efficiency (WUE, μmol CO_2 $mmol$ H_2O^{-1}) was calculated as the ratio between net photosynthetic rates and transpiration rates, and the ratio of substomatal and ambient CO_2 concentration, C_i/C_a, was determined. All measurements were performed using fully developed leaves.

Chl a fluorescence measurements and application of the JIP-test

The Chl *a* fluorescence was measured using a Handy PEA direct fluorometer (Hansatech Instruments, Norfolk, UK) on the same days, hours, and leaves as those used for steady state gas exchange measurements. After a dark adaptation period of 40 min, obtained using specific leaf clips, the measured leaves were exposed to a saturating red light pulse (peak 650 nm) of 3000 μmol photons m^{-2} s^{-1}, for 1 s, thereby generating a fluorescence transient (FT). The FT, plotted on a logarithmic timescale, showed a polyphasic behaviour, the different steps of which corresponded to a specific stage in the electron chain between reaction centres of photosystem

II (PSII) and end acceptors of photosystem I (PSI) [57,58]. The first part of the transient curve (O–J) is called 'single turnover region'. It expresses the photochemical events, providing information regarding the reduction of plastoquinone. The J–I–P region of the FT is called 'multiple turnover region' and reflects the velocity of ferredoxin reduction beyond PSI. In particular, the I–P region reflects the velocity and quantity of ferredoxin and NADP reduction via electron donation of PSI. The JIP-test was applied to the FT, and the following parameters were calculated from each curve:

- φ_{Po}: maximum quantum yield of primary photochemistry expresses the probability that an absorbed photon will be trapped by the PSII reaction centre;

- J-phase: expression of the efficiency with which a trapped exciton can move an electron into the electron transport chain from plastoquinone to the intersystem electron acceptors;

- IP-phase: expression of the efficiency of electron transport around PSI to reduce the final acceptors of the electron transport chain, i.e. ferredoxin and $NADP^+$

- PI_{tot}: a multiparametric expression that synthesizes the potential for energy conservation from photons absorbed by PSII to the reduction of PSI end acceptors.

P_N/C_i response curves

The response of net photosynthesis to the variation of substomatal CO_2 concentration was measured on the same leaves used for steady state gas exchange. Two intercalibrated CIRAS2 were used for simultaneous measurements in *F. ornus* and *Q. ilex*. The P_N/C_i curves were constructed following Long and Bernacchi, 2003 [59]. Cuvette environment was maintained at 60% relative humidity and 25°C; photosynthetic active radiation was mantained at the saturating value of 1000 μmol m^{-2}s^{-1}. The assimilation rate under CO_2 saturation (P_{Nmax}) was measured and the maximum electron transport rate driving regeneration of ribulose 1,5-bisphosphate (J_{max}, mol m^{-2} s^{-1}) was calculated according to Loustau et al. 1999 [60]. The CO_2 compensation point Γ (ppm) was derived and the *in vivo* apparent Rubisco activity (V_{cmax}, mol m^{-2}s^{-1}) was calculated as the angular coefficient of the linear part of the curve. Data at very low [CO_2], which can be limited by Rubisco deactivation, were excluded from the analysis [61].

Leaf chemistry and derivation of the photosynthetic nitrogen use efficiency

The total leaf nitrogen and carbon concentrations (N_L, C_L, % dry mass) were determined using the Dumas micro-combustion technique (Eurovector EA 3000; Milan, Italy) on the same dried leaf samples used for the calculation of sclerophylly degree (see paragraph Leaf structural and total biomass traits). Samples were ground in liquid nitrogen, and five subsamples were weighed using a precision balance (MJ-300; d = 0.001g) before the analysis. photosynthetic nitrogen-use efficiency (PNUE) was calculated as the ratio of instantaneous P_{Nmax} to nitrogen on an area basis.

Antioxidant enzymes

Antioxidant enzyme activities were determined using fresh leaf material, which was extracted as described previously [62]. All reagents for oxidative stress detection were purchased from Sigma-Aldrich (St. Louis, MO, USA). ROS production was detected using the general oxidative stress cell-permeant 2′,7′dichlorodihydrofluorescein diacetate dye. This dye passively diffuses into the cells and interacts with endogenous esterases, which cleave the diacetate groups.

The stock solution of the dye (25 μM in DMSO) was diluted to a final concentration of 5 μM. Fluorescence was monitored using a fluorescence spectrophotometer, with an excitation wavelength of 350 nm and an emission wavelength of 600 nm. The increase in fluorescence intensity yielded the ROS quantity.

The superoxide dismutase (SOD) activity was determined using an SOD assay kit WST (Sigma–Aldrich) according to manufacturer's instructions. The SOD activity (inhibition of activity) was calculated by measuring the decrease in the colour development at 440 nm. Catalase (CAT, EC 1.11.1.6) activity was measured using a commercial CAT assay kit (Sigma–Aldrich) following manufacturer's protocol. CAT activities were calculated and expressed as a decrease in absorbance at 240 nm due to H_2O_2 consumption. The total ascorbate peroxidase (APX, EC 1.11.1.11) activity of leaves was assayed by monitoring the decrease in absorbance at 290 nm due to ascorbate oxidation [63]. The concentration of ascorbic acid (ASC) was measured as described by [64]. Briefly, total ascorbate was determined after the reduction of oxidised ascorbic acid (DHA) to ASC with 1,4-dithiothreitol, and the concentration of DHA was estimated from the difference between the total ascorbate pool (ASA plus DHA) and ASC. Glutathione (GSH) content was determined at 412 nm by using 5,5´-dithiobis(2-nitrobenzoic acid), according to the spectrophotometric method of [65].

Leaf structural traits

The degree of sclerophylly was estimated by assessing the leaf mass area (LMA, g cm^{-2}). After petiole exclusion, the leaf area was measured using Image Lab software (http://en. freedownloadman-ager.org/Windows-PC/Image-Lab.html), and after the samples were dried at 80˚C to constant weight, the leaf dry weight (g) was measured.

Statistical analysis

The effect of time on ecophysiological measurements (gas exchange and Chl a fluorescence) was analysed using repeated measurement ANOVA with nitrogen and O_3 treatments as between-subjects factors. Two-way ANOVA, with nitrogen and O_3 as fixed factors, with their interaction factor, was used to analyse the ecophysiological measurements during each sampling date (DOF1, DOF 4, DOF 7, and DOF 10), and to test the differences between treatments on the P_N/C_i curve parameters and on the biochemical and structural measurements performed at the end of the experiment. Two-way ANOVA was followed by post hoc Student–Neuman–Keuls test at $p < 0.05$ when necessary. All analyses were performed using Statistica software, version 7.0 (StatSoft, Tulsa OK, USA).

Results

Steady-state gas exchange

Advancement of time (e.g plant developmental stage) affected all the gas exchanges parameters for both species, with the exception of WUE in *F. ornus*. In this species, a significant time × nitrogen interaction was noted (Table 1A) for all parameters. The time × O_3 interaction was significant for WUE and C_i/C_a in *Q. ilex*, whereas the three-level interaction was significant for WUE and C_i/C_a in both species and for g_s only in *Q. ilex*.

In particular, comparison of the gas exchange parameters of *F. ornus* for each sampling date (Fig 1) revealed that nitrogen affected all the assayed parameters at DOF 1, with a decrease in P_N, g_s, and C_i/Ca and an increase in WUE. However, at DOF4, only P_N was affected and, at the following sampling dates, no difference from C values was found.

Table 1. Analysis of variance of the gas exchange parameters for *F. ornus* and *Q. ilex*.

Factors	*F. ornus*				*Q. ilex*			
	P_N	g_s	WUE	C_i/C_a	P_N	g_s	WUE	C_i/C_a
a) *Repeated measures ANOVA*								
Time	**0.000**	**0.003**	0.077	**0.023**	**0.001**	**0.000**	**0.000**	**0.000**
Time × N	0.058	**0.004**	**0.000**	**0.000**	0.612	0.752	0.594	0.559
Time × O₃	0.435	0.589	0.173	0.069	0.606	0.070	**0.017**	**0.047**
Time × N × O₃	0.521	0.109	0.052	**0.025**	0.124	**0.010**	**0.005**	**0.006**
b) *Two-way ANOVA*								
DOF 1								
N	**0.033**	**0.002**	**0.000**	**0.000**	0.992	0.867	0.715	0.813
O₃	0.212	0.055	0.672	0.936	0.076	0.177	0.678	0.861
N × O₃	**0.013**	**0.008**	**0.004**	**0.005**	0.509	**0.050**	**0.036**	0.055
DOF 4								
N	**0.018**	0.071	0.640	0.370	0.256	0.299	0.335	0.355
O₃	**0.001**	0.051	0.885	0.900	**0.009**	**0.006**	**0.025**	**0.032**
N × O₃	0.050	0.202	0.970	0.670	0.151	0.469	0.505	0.560
DOF 7								
N	0.969	0.922	0.901	0.540	0.074	0.160	0.995	0.706
O₃	0.058	**0.035**	**0.022**	**0.001**	**0.029**	**0.004**	**0.026**	**0.012**
N × O₃	0.389	0.728	0.927	0.950	1.000	0.915	0.790	0.754
DOF 10								
N	0.432	0.725	0.185	0.162	0.146	0.117	0.496	0.658
O₃	**0.013**	**0.014**	0.230	0.354	**0.006**	**0.000**	**0.001**	**0.004**
N × O₃	**0.008**	0.050	0.748	0.944	0.597	0.316	0.858	0.757

Analysis of variance on the steady-state gas exchange parameters: Repeated measures ANOVA (a) and two-way ANOVA (b) of time, nitrogen, O₃, and their interaction effects are reported for each measurement date. DOF = day of fumigation. Significant *p*-value ($p < 0.05$) are marked in bold; 'quasi' significant values ($0.1 > p > 0.05$) are underlined.

O₃ began to affect P_N and g_s (-75% and -82% compared to those in the control, respectively) on DOF 4, lasting with the same order of magnitude through DOF 7 to 10. The interaction significantly affected P_N and g_s for low or high O₃ exposure (DOF 1 and 10, AOT40 254.22 and 2585.47 ppb h, respectively); the direction of the interaction remained the same, where the decrease of P_N and g_s relative to the control was less pronounced in O₃N plants than in O₃ alone.

For *Q. ilex* nitrogen led to the increase in both P_N and g_s relative to those in C (from +5% to 15% depending on DOF); however, the variability in the data led to $p > 0.05$ at each DOF (Fig 2). The main factor affecting gas exchange was O₃, entailing a decrement of P_N (-60% at DOF 4, - 28% at DOF 7 and -23% at DOF10) because of stomatal limitation as indicated by C_i/C_a reduction. The interaction was present on DOF 1, for low O₃ exposure (AOT40 254.22 ppb h) only for g_s, where the reduction in O₃N experimental set was higher than in the O₃ set. At DOF 4 and DOF 10, the reduction of P_N and g_s in O₃N was less pronounced than that in O₃, even if the interaction effect was not significant (Table 1B).

## *Chl a* fluorescence measurements

The repeated measures ANOVA showed that the photosystems functionality was not affected by time in both species (Table 2A).
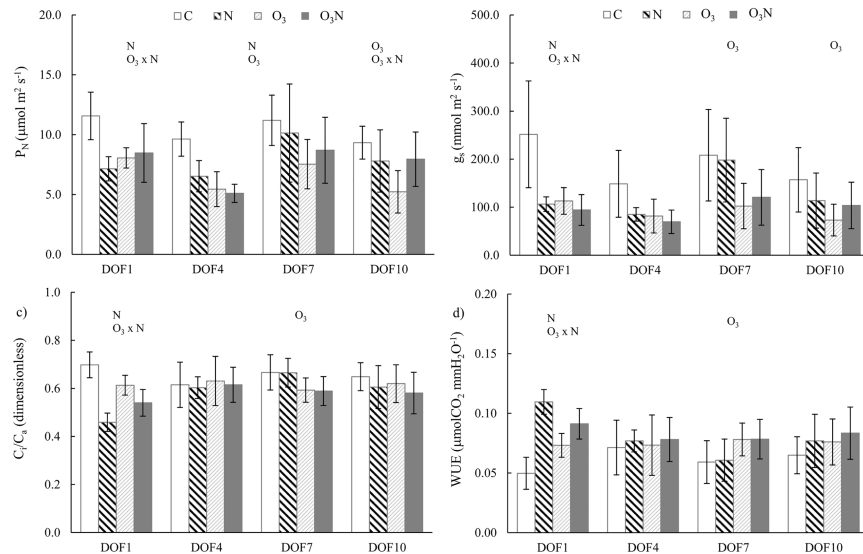
Fig 1. Trend of steady-state gas exchange parameters in *F. ornus*. The trend is shown as the mean and standard deviation (n = 5) for each treatment. Measurements were performed at the first, fourth, seventh, and tenth day of fumigation (DOF). Symbols over the bars indicate the significant factors ($p < 0.05$) affecting the gas exchange parameters: N, nitrogen effect; O_3, ozone effect; $O_3 \times N$, interaction.

In *F. ornus*, nitrogen enhanced the primary reactions characterizing the single turnover region of the fluorescence transient (Fig 3A and 3B). A slight, but significant increase of φ_{Po} occurred at DOF 4 and DOF 10, and the J-phase was affected from DOF 1 to DOF 7 (Table 2B). Nitrogen influenced the IP-phase (rate of reduction of end acceptors ferredoxin and NADP) on DOF 4 and 10 and the overall functionality of photosystems as showed by the trend of PI_{tot}. O_3 affected the JIP-test parameters since DOF 1, decreasing both IP-phase and
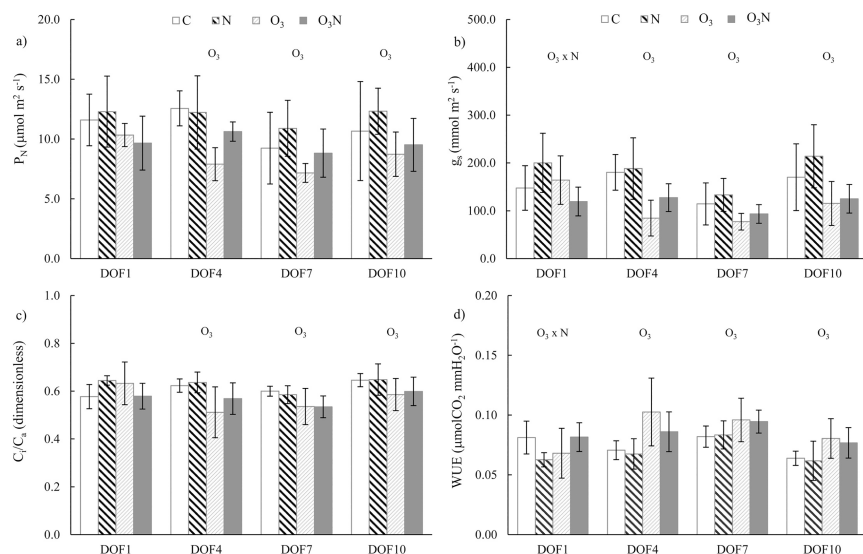
Fig 2. Trend of steady-state gas exchange parameters in *Q. ilex*. The trend is shown as the mean and standard deviation (n = 5) for each treatment. Measurements were performed at the first, fourth, seventh, and tenth day of fumigation (DOF). Symbols over the bars indicate the significant factors ($p < 0.05$) affecting the gas exchange parameters: N, nitrogen effect; O_3, ozone effect; $O_3 \times N$, interaction.

Table 2. Analysis of variance of JIP-test parameters for *F. ornus* and *Q. ilex*.

	F. ornus				*Q. ilex*			
Factors	φ_{P0}	**J-phase**	**IP-phase**	**PI$_{tot}$**	φ_{P0}	**J-phase**	**IP-phase**	**PI$_{tot}$**
a) *Repeated measures ANOVA*								
Time	0.576	0.781	<u>0.082</u>	0.141	0.249	0.369	0.363	0.419
Time × N	0.670	0.959	0.359	0.250	0.739	0.753	0.565	0.286
Time × O$_3$	0.853	0.979	0.832	0.478	0.879	0.604	0.662	0.521
Time × N × O$_3$	0.062	0.588	0.092	0.220	0.184	0.204	0.788	0.670
b) *Two-way ANOVA*								
DOF 1								
N	0.016	**0.000**	0.075	**0.000**	0.788	0.213	**0.044**	**0.044**
O$_3$	0.625	**0.004**	0.726	**0.005**	0.118	0.077	**0.001**	**0.002**
N × O$_3$	0.683	0.589	0.321	0.361	0.630	0.870	**0.016**	0.156
DOF 4								
N	**0.000**	**0.042**	**0.000**	**0.000**	0.987	0.991	0.973	0.816
O$_3$	**0.000**	0.570	0.443	**0.1**	0.022	0.365	**0.002**	**0.001**
N × O$_3$	0.552	0.435	**0.000**	**0.000**	0.521	0.313	0.789	0.776
DOF 7								
N	0.072	**0.025**	**0.056**	**0.028**	0.734	0.114	0.151	0.209
O$_3$	0.467	0.781	0.267	0.187	0.056	**0.013**	**0.001**	**0.001**
N × O$_3$	0.064	**0.014**	0.456	0.820	0.126	0.268	0.936	0.282
DOF 10								
N	**0.038**	0.765	**0.000**	**0.000**	0.744	0.374	0.834	0.178
O$_3$	0.795	0.179	**0.016**	0.114	0.195	**0.053**	**0.003**	**0.000**
N × O$_3$	0.239	0.723	**0.009**	**0.001**	0.436	0.642	0.424	0.397

Analysis of variance on JIP-test parameters: Repeated measures ANOVA (a) and two-way ANOVA (b) of time, nitrogen, O$_3$, and their interaction effects, reported for each measurement date. DOF = day of fumigation. Significant p-value ($p < 0.05$) are marked in bold; 'quasi' significant values ($0.1 > p > 0.05$) are underlined.

https://doi.org/10.1371/journal.pone.0185836.t002

Fig 3. Trend of JIP-test parameters in *F. ornus*. The histograms indicate the percentage variation of each parameter of all treatments in relation to those in control plants. Measurements were performed at the first, fourth, seventh, and tenth day of fumigation (DOF). Symbols over the bars indicate the significant factors ($p < 0.05$) affecting the gas exchange parameters: N, nitrogen effect; O$_3$, ozone effect; O$_3$ × N, interaction.
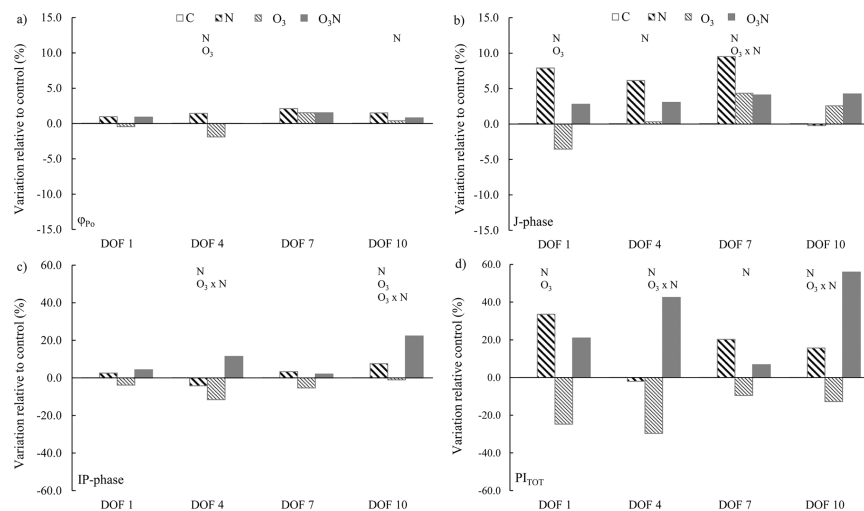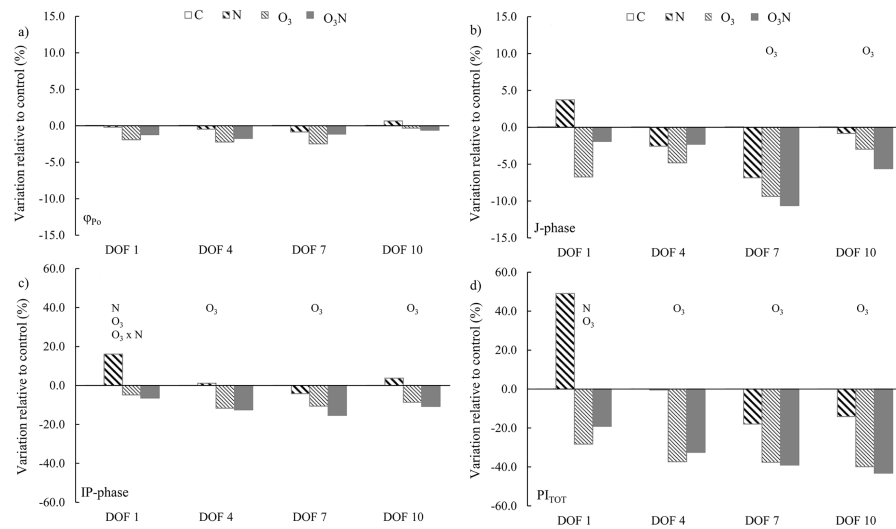
https://doi.org/10.1371/journal.pone.0185836.g003

Fig 4. Trend of JIP-test parameters in _Q. ilex_. The histograms indicate the relative variation of each parameter of all treatments in relation to those in control plants. Measurements were performed at the first, fourth, seventh, and tenth day of fumigation (DOF). Symbols over the bars indicate the significant factors ($p < 0.05$) affecting the gas exchange parameters: N, nitrogen effect; O_3, ozone effect; $O_3 \times$ N, interaction.

https://doi.org/10.1371/journal.pone.0185836.g004

PI_{tot} relative to those in the control. The interaction between nitrogen and O_3 was evident on PI_{tot} (DOF 4, 10), with nitrogen ameliorating the detrimental effect of O_3 photosystem functionality (Fig 3D).

In _Q. ilex_, the effect of nitrogen and interaction between factors on photosystems functionality was marginal (Fig 4; Table 2), affecting IP-phase and PI_{tot} on DOF1 only. The main driver of photosystem functionality was O_3, which influenced the primary photochemistry (Fig 4B) only during the final phase of O_3 exposure (DOF 7 and 10), whereas IP-phase and PI_{tot} (Fig 4C and 4D) were affected by O_3 since DOF1.

P_N/C_i response curves, leaf chemistry, and structural traits

The parameters derived from P_N/C_i curves, together with PNUE, chemical and structural leaf traits such as nitrogen and carbon concentration for the two species (N_L; C_L), their ratio, and LMA are shown in Table 3.

In _F. ornus_, P_{Nmax} increased significantly after nitrogen addition (final dose, 20 kg N ha^{-1} yr^{-1}), decreasing in response to O_3 (Table 3). The nitrogen concentration at the leaf level increased in the N experimental set, although slightly significantly ($p = 0.058$). The main driver of photosynthesis was O_3, leading to a reduction of P_{Nmax}, V_{cmax} and J_{max} relative to those in C plants. The N_L decreased because of O_3 fumigation, entailing a significant change in the C_L/N_L ratio. The interaction between factors significantly affected J_{max}: O_3 limited the positive effect of nitrogen. In _F. ornus_, nitrogen did not affect the LMA, whereas this parameter was reduced by O_3 (Table 3).

Interestingly, in _Q. ilex_, the response curves parameters were affected by nitrogen, thereby enhancing P_{Nmax} as well as the apparent maximum electron transport rate contributing to RuBP regeneration (J_{max}). Nitrogen addition resulted in an increase of N_L (+14% and +8% in N and O_3N experimental sets, respectively); however, because of high variability in the data, no significant nitrogen effect ($p > 0.05$) was detected. However, C_L significantly increased in the evergreen species.

Table 3. Parameters derived from the P_N/Ci response curves performed at the end of the experimental period and the chemical and structural leaf traits.

	F. ornus				p		
Parameters	C	N	O$_3$	O$_3$N	N	O$_3$	O$_3$N
P$_{Nmax}$	25.64 ± 4.40	32.23 ± 4.24	22.73 ± 0.19	22.14 ± 3.65	**0.015**	**0.01**	0.09
V$_{cmax}$	0.078 ± 0.01	0.067 ± 0.01	0.051 ± 0.00	0.057 ± 0.01	0.742	**0.03**	0.23
J$_{max}$	106.6 ± 18.44	136.5 ± 13.93	98.32 ± 6.26	91.58 ± 15.58	**0.012**	**0.01**	**0.04**
Γ	48.67 ± 3.68	56.2 ± 18.02	70.65 ± 23.13	52.20 ± 1.68	0.555	0.34	0.18
PNUE	1.9 ± 0.64	1.55 ± 0.28	1.40 ± 0.44	2.19 ± 1.07	0.59	0.86	0.19
N$_L$	1.71 ± 0.09	2.14 ± 0.45	1.26 ± 0.1	1.56 ± 0.32	<u>0.058</u>	**0.01**	0.71
C$_L$	44.73 ± 0.27	45.31 ± 0.6	44.25 ± 0.45	44.66 ± 0.42	0.094	<u>0.06</u>	0.76
C$_L$/N$_L$	26.15 ± 1.21	21.7 ± 3.97	35.21 ± 2.75	29.49 ± 6.66	0.067	**0.01**	0.8
LMA	0.013 ± 0.001	0.013 ± 0.001	0.011 ± 0.001	0.012±0.001	0.081	**0.003**	0.539
	Q. ilex				p		
	C	N	O$_3$	O$_3$N	N	O$_3$	O$_3$N
P$_{Nmax}$	24.73 ± 3.91	29.9 ± 1.50	23.54 ± 5.41	28.67 ± 3.10	**0.003**	0.370	0.989
V$_{cmax}$	0.076 ± 0.01	0.086 ± 0.009	0.074 ± 0.014	0.10 ± 0.017	<u>0.059</u>	0.498	0.368
J$_{max}$	105.9 ± 12.72	125.8 ± 4.19	102.3 ± 0.99	129.7 ± 8.64	**0.000**	0.982	0.438
Γ	67.69 ± 1.67	60.06 ± 13.14	67.11 ± 1.92	74.36 ± 12.98	0.972	0.238	0.204
PNUE	3.44 ± 0.97	3.00 ± 0.94	1.84 ± 0.13	2.2 ± 0.54	0.925	**0.021**	0.372
N$_L$	1.26 ± 0.14	1.44 ± 0.35	1.14 ± 0.07	1.36 ± 0.23	0.158	0.479	0.888
C$_L$	44.43 ± 0.48	45.24 ± 0.37	45.28 ± 0.21	45.55 ± 0.35	**0.036**	**0.026**	0.243
C$_L$/N$_L$	35.6 3± 4.03	32.57 ± 7.51	39.79 ± 2.36	34.01 ± 5.45	0.178	0.378	0.663
LMA	0.014 ± 0.001	0.013 ± 0.001	0.015 ± 0.001	0.012 ± 0.001	**0.000**	0.98	**0.01**

P_{Nmax}, (µmol m^{-2} s^{-1}) = maximum rate of net photosynthesis; V_{cmax}, (mol m^{-2} s^{-1}) = in vivo apparent Rubisco activity; J_{max}, (µmol m^{-2} s^{-1}) = maximum rate of electron transport; Γ, (ppm) = CO_2 compensation point; PNUE, photosynthetic nitrogen use efficiency (µmol mol^{-1} s^{-1}); N_L, nitrogen at leaf level (%); C_L, carbon concentration at leaf level (%); C_L/N_L, ratio between carbon and nitrogen at leaf level; Leaf Mass Area (LMA, g cm^{-2}). Data are shown as the mean ± standard deviation (n = 5) for each treatment. On the right panel, results of two-way ANOVA for each parameter are shown. Significant p-value ($p < 0.05$) are marked in bold; quasi 'significant' values ($0.1 > p > 0.05$) are underlined.

O_3 caused the reduction in PNUE, because of slight, but not significant ($p > 0.05$), reduction of P_{Nmax} and N_L, and an increase in C_L concentration. No interaction was detected. LMA decreased in *Q. ilex* after nitrogen addition, because leaf area increased (data not shown), influencing in the same direction as the LMA of the O_3N experimental set.

Antioxidant enzyme activities

In both species, nitrogen addition increased SOD, CAT, and GSH activities, the key enzymatic components of the first antioxidant defense mechanisms involved in O_2^- and H_2O_2 scavenging (Fig 5).

In *F. ornus*, the ROS amount increased significantly under O_3 exposure; however, compared to that in C, their concentration in the O_3 experimental set was higher than that in the O_3N experimental set. Accordingly, the activity of the first line of ROS scavengers such as SOD and CAT were higher in O_3 than in the O_3N experimental set, but the antioxidants involved in the conversion of H_2O_2 to O_2 or H_2O (i.e. APX, ASA, DHA, and GSH) were upregulated in the O_3N plants. Conversely, in *Q. ilex*, even if ROS were produced to the same extent as in O_3 and O_3N plants, SOD and CAT were lower in O_3N than in O_3. All the antioxidants related to ascorbate-glutathione cycle were higher in O_3N than in O_3 plants.
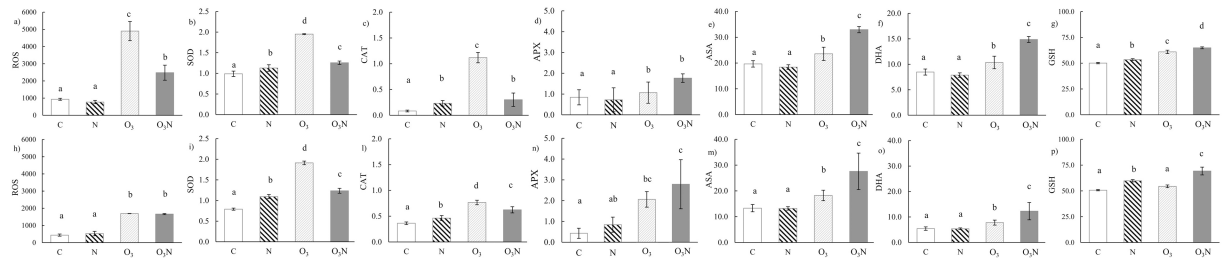
Fig 5. The outputs of biochemical analysis. They are shown for each treatment at the end of the experimental period for *F. ornus* (upper panel, from a to g) and *Q. ilex* (below panel, from h to p). Reactive oxygen species (ROS, %); superoxide dismutase, (SOD, inhibition rate %); catalase (CAT, U mg^{-1} of protein); ascorbate peroxidase (APX, U mg^{-1} of protein); total concentration of ascorbic acid (ASA, mg g^{-1}); oxidised ascorbic acid (DHA, mg g^{-1}); and glutathione (GSH, mg g^{-1}). Data are means ± standard deviation (n = 5), and bars not accompanied by the same letter are significantly different at *p* < 0.05, by using post hoc Student–Neuman–Keuls test.

https://doi.org/10.1371/journal.pone.0185836.g005

Discussion

The impacts of atmospheric nitrogen deposition and O_3 on Mediterranean forests have been of increasing concern, and experimental data are needed to elucidate the mechanisms of action, or identify specific functional traits affected by interacting stress factors. Thus, the present study aimed to measure the effects of realistic exposure of nitrogen and O_3 on a broad range of traits of two Mediterranean species with different leaf habits, to characterize their response. The study was performed under controlled condition in a medium-term experiment, in order to determine the traits that are first affected by nitrogen and how the potential nitrogen effects can influence the response to O_3. Moreover, to our knowledge, this is the first study to compare *F. ornus* and *Q. ilex* directly after O_3 exposure, with important implication for assessing the risk for these co-occurring species.

Response patterns to nitrogen deposition

An overview of available literature highlights that the results for the effects of nitrogen deposition at the leaf and plant levels are contradictory [37,66]. The numerous processes involved in nitrogen assimilation and metabolism might lead to high variability in the assayed data. In our experiment, after an acclimation period to nitrogen, when the cumulative dose was roughly equivalent to 14 kg N ha yr^{-1}, which was within the threshold load considered as critical for Mediterranean vegetation, nitrogen concentration at the leaf level did not increase in both species, and no adverse effect was detected on photosynthetic traits (data not shown). When nitrogen exposure exceeded this level, between 14 and 17 kg N ha yr^{-1} (DOF 1), assimilation rate measured under steady state conditions was adversely affected in *F. ornus* possibly because of the nitrogen-induced decrease in stomatal conductance, as documented in several species [67,68]. Indeed nitrogen can affect g_s by changing the hydraulic conductivity [40], or by increasing nitric oxide (NO) emission as a side-reaction of the nitrate assimilation process [69]. In fact, NO is involved in the ABA-induced stomatal closure process [68,70]. Since the first mechanism was observed in long-lasting fertilisation experiments (from 2 to 5 years of nitrogen addition), we argued that, in our study, the nitrogen effect on g_s could be mediated by NO signalling.

Interestingly, in both species, P_{Nmax} and J_{max} increased because of nitrogen, whereas V_{cmax} did not change, namely, the electron transport driving RuBP regeneration was more affected than carboxylation. This result also explains why the assimilation rate measured under steady state condition, i.e. in the Rubisco-limited phase [59], did not show variations. Moreover, this

evidence and the Chl a fluorescence measurement, indicate that, in $Q.\ ilex$, a higher fraction of nitrogen was allocated to components related to biochemical phase of assimilation process than to light-harvesting elements [71]. This hypothesis is not completely applicable to $F.\ ornus$. In fact, in $Q.\ ilex$, nitrogen significantly affects only the parameters related to the functionality of the end acceptors (i.e. IP-phase and PI_{tot}); in contrast in $F.\ ornus$ primary photochemistry (φ_{Po} and J-phase) was also enhanced by nitrogen, confirming that the partitioning pattern can differ depending on leaf habit [47].

In agreement with ecophysiological measurements, at the end of the experimental period, the concentration of nitrogen on mass basis increased to a different extent between the species. In $F.\ ornus$, nitrogen addition resulted in 25% higher N_L relative to that in the control ($p = 0.058$), whereas in $Q.\ ilex$ the variation was less pronounced (+ 14%). Notably in both species PNUE did not change because of nitrogen addition. PNUE is controlled by physiological (assimilation rate, Rubisco activity, and nitrogen concentration on area basis) and structural traits (LMA, leaf thickness) [72], which can change in opposite ways and explain the lack of difference among treatments. In $F.\ ornus$, nitrogen treatment decreased both leaf area and dry mass, resulting in no LMA variation. However, in $Q.\ ilex$, the LMA decreased because of nitrogen, since the leaf area increased; thus, the evergreen species did not invest resources in the cell wall to increase leaf toughness, as reported in other studies [73,74].

These effects of nitrogen supply on leaf structural traits could influence the leaf nitrogen concentration when it is considered on area-basis [28,75]. In $F.\ ornus$, area-based leaf nitrogen was lower relative to the mass-based value (data not shown), whereas the two values remained similar in $Q.\ ilex$.

Response patterns to ozone

Ozone effect was assessed using a wide range of traits to allow defining thoroughly the differences in the response patterns between the species. Plant sensitivity to O_3 cannot be identified based on the extent of leaf injury alone, because impairments to photosystem functionality and photochemistry occur before the appearance of visible injury [54,76]. In our experiment, although we adopted a realistic O_3 exposure (80 ppb h, AOT40 2458), $F.\ ornus$ seemed to be sensitive to this pollutant because it did not trigger an active physiological response to O_3, such as avoidance mechanisms, activating instead an incoming injury. The gas exchange reduction occurred from the first day of fumigation (-55% and -33% for g_s and P_N, respectively), remaining around this order of magnitude for the entire fumigation period. Furthermore, in this species the P_N reduction was not merely owing to stomatal limitation, since the P_N/Ci response curves highlighted a decrease of P_{Nmax} and of both carboxylation efficiency (V_{cmax}) and maximum electron transport rate driving RuBP regeneration (J_{max}). The reduction of nitrogen concentration can also be a good indicator of O_3 injury, helping to define the scale of tolerance between species [23]. In $F.\ ornus$, O_3 exposure accelerated the processes related to senescence as shown by the decrease of leaf nitrogen and dry matter i.e. decrease of LMA. Although the results from controlled conditions cannot be extended to natural ecosystems, the sensitivity found in this experiment should be considered for risk assessment of tree species in a Mediterranean climate. The response pattern of $Q.\ ilex$ to O_3 can be attributed to an avoidance mechanism, as shown by traits related to photochemistry, photosystems functionality or structural traits. The reduction of P_N in O_3-treated plants relative to controls was less pronounced in $Q.\ ilex$ than in $F.\ ornus$, starting on DOF 4, and was related to stomatal limitation more than to biochemical impairments. Indeed, the parameters derived from P_N/Ci curves did not indicate any detrimental effect on Rubisco activity because of O_3, whereas the analysis of photosystem functionality highlighted a down-regulation mechanisms (i.e. reduction of end-acceptors

activity). The differences in the response strategies implemented by the two species could be strictly associated with a different antioxidant potential [11]. Indeed, the inherent amount of CAT, responsible for the removal of H_2O_2 [77], was higher in *Q. ilex*. Moreover, the components involved in the ascorbate-glutathione cycle (APX, ASA, DHA, and GSH) showed high concentration or activity in *Q. ilex* relative to that in *F. ornus*, but these could be related to the higher stomatal conductance (that is, high O_3 fluxes) in the former species. Furthermore, in both the species, the finding that, in O_3-treated plants, the increase in DHA/ASA ratio was lower than the increases in APX activity, suggesting that recycling of DHA to ASA was not compromised by O_3.

Response patterns to the interaction between nitrogen deposition and ozone

Information on the interactive effects of nitrogen deposition and ozone pollution on vegetation is still scarce [34]. Many of the studies on nitrogen and O_3 have focused on the changes in community structure or species abundance in grasslands ecosystems [30,31,78]. However, few studies have determined the consequences of nitrogen and O_3 interaction on tree species [24,38,43]. The results highlighted by previous studies suggested that the interactive effects could be dynamic, changing throughout the growing season, and the effects on key ecophysiological parameters such as P_N and g_s can remarkably change depending on the concentration of nitrogen and O_3 exposure. In the present study, the interaction followed different patterns in the two species, confirming our hypothesis that leaf habit plays a crucial role in determining the way of interaction between the two factors. In particular, in *F. ornus*, the interaction was detectable on several traits indicating that nitrogen addition can ameliorate the detrimental effects owing to O_3. Nitrogen had a positive effect on the processes related to photochemistry, resulting in enhanced carbon assimilation rate in the O_3N experimental set relative to that in the O_3 experimental set. The mechanisms involved in this type of response could be associated with the investment of available nitrogen to proteins that play a crucial role in enhancing the photosynthetic activity [79]. We argue that nitrogen was partially allocated to light-harvesting components, increasing the capacity to manage the energy flow through the photosystems even if stomatal closure occurs [57]. The positive effect of nitrogen on the functionality of plants treated with O_3 could also be attributed to the upregulation of antioxidant response to O_3 implemented by nitrogen addition [80]. In particular, in O_3N plants, the APX activity and ASA and DHA were higher compared to that after treatment with O_3 alone. Moreover, in *F. ornus*, the O_3N experimental set led to lower ROS production relative to that in O_3 plants, that is, lower exposure to oxidative stress, even if the O_3 fluxes remained almost the same. On average, during the entire experimental period, g_s was about 96.9 ± 21.2 and 92.5 ± 12.3 in O_3 and O_3N, respectively. This could be because of NO synthesis. Plants can emit NO under a series of stresses [81], in particular under ozone exposure [7], and several studies revealed that high nitrogen availability can promote NO production [82]. NO is involved in triggering antioxidant response and can react directly with free radicals such as H_2O_2 and O_2^-, thereby decreasing their concentrations. We argue that, in the presence of high nitrogen availability, *F. ornus* can cope with incoming oxidative stress via the production of NO, which owing to the rapid synthesis and prompt availability, allows prompt scavenging of free radicals and concomitantly increases the photosynthesis rate [83]. As shown by Velikova et al. [78], higher NO is emitted in isoprene-inhibited leaves; therefore NO synthesis should be favoured in plants that do not emit VOCs, such as *F. ornus*. In *Q. ilex*, a strong monoterpene emitter species [84], the response to oxidative compounds could be attributed to VOCs [85] rather than to NO. Most importantly, in both species, nitrogen led to the increase in the constitutive amount of

antioxidant enzymes such as SOD and CAT, but did not affect their activity (GST did not change, data not shown).

Unlike in *F. ornus*, in *Q. ilex*, the interaction between nitrogen and O_3 was weak and appeared only on DOF 1, when nitrogen seemed to aggravate the stomatal limitation owing to O_3. The g_s of O_3N plants recovered at the following sampling times to the level in the O_3 experimental set.

Photosystem functionality was not affected by the interaction, and Rubisco-related parameters did not show any nitrogen effect (positive or negative) when plants were exposed to O_3. However, interestingly, enzymes such as SOD and CAT, which play a crucial role in determining a suitable level of ROS in different cell compartments [77], were lower in O_3N plants than in O_3 plants, although the ROS production did not differ between the treatments. This evidence suggests that, in *Q. ilex*, nitrogen addition could enhance secondary metabolism and promote the production of VOCs that can directly quench O_3 without activating an enzymatic antioxidant response. Conversely, similar to that in *F. ornus*, nitrogen upregulated the activity of the ascorbate-glutathione cycle in *Q. ilex*, indicating that nitrogen deposition can largely protect against oxidative stressors and to multi-stress condition experienced by Mediterranean vegetation.

Conclusion

In both species, photosynthetic traits such as photosystem functionality, maximum assimilation and maximum electron transport rate were enhanced by nitrogen at the end of the experiment, when 20 kg N ha^{-1} y^{-1} had been reached. Moreover, in both species, nitrogen enhanced the constitutive level of antioxidant activity, thus with a potential ameliorative effect on O_3-related impacts. In *F. ornus* nitrogen was allocated to the light harvesting components as shown by chlorophyll *a* fluorescence measurements. The results suggest that *F. ornus* is an O_3-sensitive species, as shown by biochemical limitation to photosynthesis and the acceleration of leaf senescence-related processes. In *F. ornus*, nitrogen ameliorated the detrimental effects that O_3 had on the photosynthetic processes. The interaction between nitrogen and O_3 had different mechanisms of action in the two species. In the deciduous species *F. ornus*, the lower ROS production in the interaction experimental set (O_3N) might be related to the enhanced nitrogen oxide production, whereas, in *Q. ilex*, nitrogen might have upregulated the secondary metabolism, promoting high VOCs production. This hypothesis is based on the fact that, although no difference was noted in ROS production between O_3 and O_3N plants in this species, the activity of the first-level scavenging enzymes such SOD or CAT was lower in the interaction experimental set. These results indicate that nitrogen deposition could counteract the detrimental effect of O_3, thus suggesting that nitrogen is an important factor for assessing the critical level of O_3 for Mediterranean vegetation.

Acknowledgments

Author Contributions

Conceptualization: Lina Fusaro.

Data curation: Lina Fusaro, Elisabetta Salvatori.

Formal analysis: Lina Fusaro, Adriano Palma, Adriana Basile, Viviana Maresca, Elham Asadi Karam.

Funding acquisition: Fausto Manes.

Methodology: Lina Fusaro.

Supervision: Fausto Manes.

Writing – original draft: Lina Fusaro.

Writing – review & editing: Elisabetta Salvatori, Fausto Manes.

References

1. Niinemets Ü. Cohort-specific tuning of foliage physiology to interacting stresses in evergreens. Tree Physiol. 2014; 34: 1301–1304. https://doi.org/10.1093/treephys/tpu099 PMID: 25428824

2. Mills G, Harmens H, Wagg S, Sharps K, Hayes F, Fowler D, et al. Ozone impacts on vegetation in a nitrogen enriched and changing climate. Environ Pollut. 2016; 208, Part B: 898–908. https://doi.org/10.1016/j.envpol.2015.09.038

3. Manual on Methodologies and Criteria for Modelling and Mapping Critical Loads and Levels and Air Pollution Effects, Risks and Trends—European Environment Agency [Internet]. [cited 26 Apr 2017]. http://www.eea.europa.eu/data-and-maps/indicators/exposure-of-ecosystems-to-acidification-2/manual-on-methodologies-and-criteria

4. Santurtún A, González-Hidalgo JC, Sanchez-Lorenzo A, Zarrabeitia MT. Surface ozone concentration trends and its relationship with weather types in Spain (2001–2010). Atmos Environ. 2015; 101: 10–22. https://doi.org/10.1016/j.atmosenv.2014.11.005

5. Bytnerowicz A, Omasa K, Paoletti E. Integrated effects of air pollution and climate change on forests: A northern hemisphere perspective. Environ Pollut. 2007; 147: 438–445. https://doi.org/10.1016/j.envpol.2006.08.028 PMID: 17034915

6. de Vries W, Dobbertin MH, Solberg S, van Dobben HF, Schaub M. Impacts of acid deposition, ozone exposure and weather conditions on forest ecosystems in Europe: an overview. Plant Soil. 2014; 380: 1–45. https://doi.org/10.1007/s11104-014-2056-2

7. Vainonen JP, Kangasjärvi J. Plant signalling in acute ozone exposure. Plant Cell Environ. 2015; 38: 240–252. https://doi.org/10.1111/pce.12273 PMID: 24417414

8. Das P, Nutan KK, Singla-Pareek SL, Pareek A. Oxidative environment and redox homeostasis in plants: dissecting out significant contribution of major cellular organelles. Front Environ Sci. 2015; 2. https://doi.org/10.3389/fenvs.2014.00070

9. Cotrozzi L, Remorini D, Pellegrini E, Landi M, Massai R, Nali C, et al. Variations in physiological and biochemical traits of oak seedlings grown under drought and ozone stress. Physiol Plant. 2016; 157: 69–84. https://doi.org/10.1111/ppl.12402 PMID: 26541269

10. Guidi L, Degl'Innocenti E, Giordano C, Biricolti S, Tattini M. Ozone tolerance in Phaseolus vulgaris depends on more than one mechanism. Environ Pollut. 2010; 158: 3164–3171. https://doi.org/10.1016/j.envpol.2010.06.037 PMID: 20656389

11. Nali C, Paoletti E, Marabottini R, Della Rocca G, Lorenzini G, Paolacci AR, et al. Ecophysiological and biochemical strategies of response to ozone in Mediterranean evergreen broadleaf species. Atmos Environ. 2004; 38: 2247–2257. https://doi.org/10.1016/j.atmosenv.2003.11.043

12. Scalet M, Federico R, Guido MC, Manes F. Peroxidase activity and polyamine changes in response to ozone and simulated acid rain in Aleppo pine needles. Environ Exp Bot. 1995; 35: 417–425. https://doi.org/10.1016/0098-8472(95)00001-3

13. Calatayud V, Cerveró J, Sanz MJ. Foliar, Physiologial and Growth Responses of Four Maple Species Exposed to Ozone. Water Air Soil Pollut. 2007; 185: 239–254. https://doi.org/10.1007/s11270-007-9446-5

14. Mills G, Hayes F, Wilkinson S, Davies WJ. Chronic exposure to increasing background ozone impairs stomatal functioning in grassland species. Glob Change Biol. 2009; 15: 1522–1533. https://doi.org/10.1111/j.1365-2486.2008.01798.x

15. Fusaro L, Gerosa G, Salvatori E, Marzuoli R, Monga R, Kuzminsky E, et al. Early and late adjustments of the photosynthetic traits and stomatal density in Quercus ilex L. grown in an ozone-enriched environment. Plant Biol. 2016; 18: 13–21. https://doi.org/10.1111/plb.12383 PMID: 26307426

16. Calatayud V, Cerveró J, Calvo E, García-Breijo F-J, Reig-Armiñana J, Sanz MJ. Responses of evergreen and deciduous Quercus species to enhanced ozone levels. Environ Pollut. 2011; 159: 55–63. https://doi.org/10.1016/j.envpol.2010.09.024 PMID: 20974507

17. Manes F, Donato E, Vitale M. Physiological response of Pinus halepensis needles under ozone and water stress conditions. Physiol Plant. 2001; 113: 249–257. https://doi.org/10.1034/j.1399-3054.2001.1130213.x PMID: 12060303

18. Ribas À, Peñuelas J, Elvira S, Gimeno BS. Contrasting effects of ozone under different water supplies in two Mediterranean tree species. Atmos Environ. 2005; 39: 685–693. https://doi.org/10.1016/j.atmosenv.2004.10.022

19. Bussotti F. Functional leaf traits, plant communities and acclimation processes in relation to oxidative stress in trees: a critical overview. Glob Change Biol. 2008; 14: 2727–2739. https://doi.org/10.1111/j.1365-2486.2008.01677.x

20. Li P, Calatayud V, Gao F, Uddling J, Feng Z. Differences in ozone sensitivity among woody species are related to leaf morphology and antioxidant levels. Tree Physiol. 2016; 36: 1105–1116. https://doi.org/10.1093/treephys/tpw042 PMID: 27217527

21. Zhang W, Feng Z, Wang X, Niu J. Responses of native broadleaved woody species to elevated ozone in subtropical China. Environ Pollut. 2012; 163: 149–157. https://doi.org/10.1016/j.envpol.2011.12.035 PMID: 22325443

22. Karnosky DF, Skelly JM, Percy KE, Chappelka AH. Perspectives regarding 50 years of research on effects of tropospheric ozone air pollution on US forests. Environ Pollut. 2007; 147: 489–506. https://doi.org/10.1016/j.envpol.2006.08.043 PMID: 17084004

23. Ribas À, Peñuelas J, Elvira S, Gimeno BS. Ozone exposure induces the activation of leaf senescence-related processes and morphological and growth changes in seedlings of Mediterranean tree species. Environ Pollut. 2005; 134: 291–300. https://doi.org/10.1016/j.envpol.2004.07.026 PMID: 15589656

24. Yamaguchi M, Watanabe M, Matsumura H, Kohno Y, Izuta T. Experimental Studies on the Effects of Ozone on Growth and Photosynthetic Activity of Japanese Forest Tree Species. Asian J Atmospheric Environ. 2011; 5: 65–78. https://doi.org/10.5572/ajae.2011.5.2.065

25. Uscola M, Oliet JA, Villar-Salvador P, Díaz-Pinés E, Jacobs DF. Nitrogen form and concentration interact to affect the performance of two ecologically distinct Mediterranean forest trees. Eur J For Res. 2014; 133: 235–246. https://doi.org/10.1007/s10342-013-0749-3

26. Bobbink R, Hicks K, Galloway J, Spranger T, Alkemade R, Ashmore M, et al. Global assessment of nitrogen deposition effects on terrestrial plant diversity: a synthesis. Ecol Appl. 2010; 20: 30–59. https://doi.org/10.1890/08-1140.1 PMID: 20349829

27. Dirnböck T, Grandin U, Bernhardt-Römermann M, Beudert B, Canullo R, Forsius M, et al. Forest floor vegetation response to nitrogen deposition in Europe. Glob Change Biol. 2014; 20: 429–440. https://doi.org/10.1111/gcb.12440

28. Fleischer K, Rebel KT, van der Molen MK, Erisman JW, Wassen MJ, van Loon EE, et al. The contribution of nitrogen deposition to the photosynthetic capacity of forests. Glob Biogeochem Cycles. 2013; 27: 187–199. https://doi.org/10.1002/gbc.20026

29. García-Gómez H, Garrido JL, Vivanco MG, Lassaletta L, Rábago I, Àvila A, et al. Nitrogen deposition in Spain: Modeled patterns and threatened habitats within the Natura 2000 network. Sci Total Environ. 2014; 485–486: 450–460. https://doi.org/10.1016/j.scitotenv.2014.03.112 PMID: 24742555

30. Volk M, Enderle J, Bassin S. Subalpine grassland carbon balance during 7 years of increased atmospheric N deposition. Biogeosciences. 2016; 13: 3807–3817. https://doi.org/10.5194/bg-13-3807-2016

31. Calvete-Sogo H, González-Fernández I, Sanz J, Elvira S, Alonso R, García-Gómez H, et al. Heterogeneous responses to ozone and nitrogen alter the species composition of Mediterranean annual pastures. Oecologia. 2016; 181: 1055–1067. https://doi.org/10.1007/s00442-016-3628-z PMID: 27106851

32. Fenn ME, Allen EB, Weiss SB, Jovan S, Geiser LH, Tonnesen GS, et al. Nitrogen critical loads and management alternatives for N-impacted ecosystems in California. J Environ Manage. 2010; 91: 2404–2423. https://doi.org/10.1016/j.jenvman.2010.07.034 PMID: 20705383

33. Pardo LH, Fenn ME, Goodale CL, Geiser LH, Driscoll CT, Allen EB, et al. Effects of nitrogen deposition and empirical nitrogen critical loads for ecoregions of the United States. Ecol Appl. 2011; 21: 3049–3082. https://doi.org/10.1890/10-2341.1

34. Ochoa-Hueso R, Munzi S, Alonso R, Arróniz-Crespo M, Avila A, Bermejo V, et al. Ecological impacts of atmospheric pollution and interactions with climate change in terrestrial ecosystems of the Mediterranean Basin: Current research and future directions. Environ Pollut. 2017; 227: 194–206. https://doi.org/10.1016/j.envpol.2017.04.062 PMID: 28460237

35. Borghetti M, Gentilesca T, Leonardi S, van Noije T, Rita A, Mencuccini M. Long-term temporal relationships between environmental conditions and xylem functional traits: a meta-analysis across a range of woody species along climatic and nitrogen deposition gradients. Tree Physiol. 2017; 37: 4–17. https://doi.org/10.1093/treephys/tpw087 PMID: 28173594

36. Camarero JJ, Carrer M, Way D. Bridging long-term wood functioning and nitrogen deposition to better understand changes in tree growth and forest productivity. Tree Physiol. 2017; 37: 1–3. https://doi.org/10.1093/treephys/tpw111 PMID: 28175915

37. Ferretti M, Marchetto A, Arisci S, Bussotti F, Calderisi M, Carnicelli S, et al. On the tracks of Nitrogen deposition effects on temperate forests at their southern European range–an observational study from Italy. Glob Change Biol. 2014; 20: 3423–3438. https://doi.org/10.1111/gcb.12552 PMID: 24729460

38. Azuchi F, Kinose Y, Matsumura T, Kanomata T, Uehara Y, Kobayashi A, et al. Modeling stomatal conductance and ozone uptake of Fagus crenata grown under different nitrogen loads. Environ Pollut. 2014; 184: 481–487. https://doi.org/10.1016/j.envpol.2013.09.025 PMID: 24134917

39. Thomas VFD, Braun S, Flückiger W. Effects of simultaneous ozone exposure and nitrogen loads on carbohydrate concentrations, biomass, and growth of young spruce trees (Picea abies). Environ Pollut. 2005; 137: 507–516. https://doi.org/10.1016/j.envpol.2005.02.002 PMID: 16005762

40. Pivovaroff AL, Santiago LS, Vourlitis GL, Grantz DA, Allen MF. Plant hydraulic responses to long-term dry season nitrogen deposition alter drought tolerance in a Mediterranean-type ecosystem. Oecologia. 2016; 181: 721–731. https://doi.org/10.1007/s00442-016-3609-2 PMID: 27017604

41. Crous KY, O'Sullivan OS, Zaragoza-Castells J, Bloomfield KJ, Negrini ACA, Meir P, et al. Nitrogen and phosphorus availabilities interact to modulate leaf trait scaling relationships across six plant functional types in a controlled-environment study. New Phytol. 2017; 215: 992–1008. https://doi.org/10.1111/nph.14591 PMID: 28505389

42. Yamaguchi M, Watanabe M, Iwasaki M, Tabe C, Matsumura H, Kohno Y, et al. Growth and photosynthetic responses of Fagus crenata seedlings to O3 under different nitrogen loads. Trees. 2007; 21: 707–718. https://doi.org/10.1007/s00468-007-0163-x

43. Marzuoli R, Monga R, Finco A, Gerosa G. Biomass and physiological responses of Quercus robur (L.) young trees during 2 years of treatments with different levels of ozone and nitrogen wet deposition. Trees. 2016; 30: 1995–2010. https://doi.org/10.1007/s00468-016-1427-0

44. Catovsky S, Bazzaz FA. Nitrogen Availability Influences Regeneration of Temperate Tree Species in the Understory Seedling Bank. Ecol Appl. 2002; 12: 1056–1070. https://doi.org/10.1890/1051-0761(2002)012[1056:NAIROT]2.0.CO;2

45. Tulloss EM, Cadenasso ML. The Effect of Nitrogen Deposition on Plant Performance and Community Structure: Is It Life Stage Specific? PLOS ONE. 2016; 11: e0156685. https://doi.org/10.1371/journal.pone.0156685 PMID: 27253718

46. Wright IJ, Reich PB, Westoby M, Ackerly DD, Baruch Z, Bongers F, et al. The worldwide leaf economics spectrum. Nature. 2004; 428: 821–827. https://doi.org/10.1038/nature02403 PMID: 15103368

47. Takashima T, Hikosaka K, Hirose T. Photosynthesis or persistence: nitrogen allocation in leaves of evergreen and deciduous Quercus species. Plant Cell Environ. 2004; 27: 1047–1054. https://doi.org/10.1111/j.1365-3040.2004.01209.x

48. Feng Y-L, Lei Y-B, Wang R-F, Callaway RM, Valiente-Banuet A, Inderjit, et al. Evolutionary tradeoffs for nitrogen allocation to photosynthesis versus cell walls in an invasive plant. Proc Natl Acad Sci. 2009; 106: 1853–1856. https://doi.org/10.1073/pnas.0808434106 PMID: 19171910

49. Tretiach M. Photosynthesis and transpiration of evergreen Mediterranean and deciduous trees in an ecotone during a growing season. Acta Oecologica. 1993; 14: 341–360.

50. Valladares F, Martinez-Ferri E, Balaguer L, Perez-Corona E, Manrique E. Low leaf-level response to light and nutrients in Mediterranean evergreen oaks: a conservative resource-use strategy? New Phytol. 2000; 148: 79–91. https://doi.org/10.1046/j.1469-8137.2000.00737.x

51. Paoletti E, Contran N, Bernasconi P, Günthardt-Goerg MS, Vollenweider P. Erratum to "Structural and physiological responses to ozone in Manna ash (Fraxinus ornus L.) leaves of seedlings and mature trees under controlled and ambient conditions" [Science of the Total Environment 407 (2009) 1631–1643]. Sci Total Environ. 2010; 408: 2013. https://doi.org/10.1016/j.scitotenv.2010.01.022

52. Manes F, Vitale M, Maria Fabi A, De Santis F, Zona D. Estimates of potential ozone stomatal uptake in mature trees of Quercus ilex in a Mediterranean climate. Environ Exp Bot. 2007; 59: 235–241. https://doi.org/10.1016/j.envexpbot.2005.12.001

53. Bazzaz FA, Carlson RW. Photosynthetic acclimation to variability in the light environment of early and late successional plants. Oecologia. 1982; 54: 313–316. https://doi.org/10.1007/BF00379999 PMID: 28309954

54. Salvatori E, Fusaro L, Strasser RJ, Bussotti F, Manes F. Effects of acute O3 stress on PSII and PSI photochemistry of sensitive and resistant snap bean genotypes (Phaseolus vulgaris L.), probed by prompt chlorophyll "a" fluorescence and 820 nm modulated reflectance. Plant Physiol Biochem. 2015; 97: 368–377. https://doi.org/10.1016/j.plaphy.2015.10.027 PMID: 26535554

55. Fares S, Schnitzhofer R, Jiang X, Guenther A, Hansel A, Loreto F. Observations of Diurnal to Weekly Variations of Monoterpene-Dominated Fluxes of Volatile Organic Compounds from Mediterranean Forests: Implications for Regional Modeling. Environ Sci Technol. 2013; 47: 11073–11082. https://doi.org/10.1021/es4022156 PMID: 24004275

56. Manes F, De Santis F, Giannini MA, Vazzana C, Capogna F, Allegrini I. Integrated ambient ozone evaluation by passive samplers and clover biomonitoring mini-stations. Sci Total Environ. 2003; 308: 133–141. https://doi.org/10.1016/S0048-9697(02)00633-2 PMID: 12738207

57. Strasser RJ, Tsimilli-Michael M, Qiang S, Goltsev V. Simultaneous in vivo recording of prompt and delayed fluorescence and 820-nm reflection changes during drying and after rehydration of the resurrection plant Haberlea rhodopensis. Biochim Biophys Acta BBA—Bioenerg. 2010; 1797: 1313–1326. https://doi.org/10.1016/j.bbabio.2010.03.008 PMID: 20226756

58. Salvatori E, Fusaro L, Gottardini E, Pollastrini M, Goltsev V, Strasser RJ, et al. Plant stress analysis: Application of prompt, delayed chlorophyll fluorescence and 820 nm modulated reflectance. Insights from independent experiments. Plant Physiol Biochem. 2014; 85: 105–113. https://doi.org/10.1016/j.plaphy.2014.11.002 PMID: 25463266

59. Long SP, Bernacchi CJ. Gas exchange measurements, what can they tell us about the underlying limitations to photosynthesis? Procedures and sources of error. J Exp Bot. 2003; 54: 2393–2401. https://doi.org/10.1093/jxb/erg262 PMID: 14512377

60. Loustau D, Brahim MB, Gaudillère J-P, Dreyer E. Photosynthetic responses to phosphorus nutrition in two-year-old maritime pine seedlings. Tree Physiol. 1999; 19: 707–715. https://doi.org/10.1093/treephys/19.11.707 PMID: 12651309

61. Sharkey TD, Bernacchi CJ, Farquhar GD, Singsaas EL. Fitting photosynthetic carbon dioxide response curves for C3 leaves. Plant Cell Environ. 2007; 30: 1035–1040. https://doi.org/10.1111/j.1365-3040.2007.01710.x PMID: 17661745

62. Guidi L, Degl'Innocenti E, Remorini D, Massai R, Tattini M. Interactions of water stress and solar irradiance on the physiology and biochemistry of Ligustrum vulgare. Tree Physiol. 2008; 28: 873–883. https://doi.org/10.1093/treephys/28.6.873 PMID: 18381268

63. Nakano Y, Asada K. Hydrogen Peroxide is Scavenged by Ascorbate-specific Peroxidase in Spinach Chloroplasts. Plant Cell Physiol. 1981; 22: 867–880. https://doi.org/10.1093/oxfordjournals.pcp.a076232

64. de Pinto MC, Francis D, Gara LD. The redox state of the ascorbate-dehydroascorbate pair as a specific sensor of cell division in tobacco BY-2 cells. Protoplasma. 1999; 209: 90–97. https://doi.org/10.1007/BF01415704 PMID: 18987797

65. Ellman GL. Tissue sulfhydryl groups. Arch Biochem Biophys. 1959; 82: 70–77. https://doi.org/10.1016/0003-9861(59)90090-6 PMID: 13650640

66. Dezi S, Medlyn BE, Tonon G, Magnani F. The effect of nitrogen deposition on forest carbon sequestration: a model-based analysis. Glob Change Biol. 2010; 16: 1470–1486. https://doi.org/10.1111/j.1365-2486.2009.02102.x

67. Amponsah IG, Lieffers VJ, Comeau PG, Brockley RP. Growth response and sapwood hydraulic properties of young lodgepole pine following repeated fertilization. Tree Physiol. 2004; 24: 1099–1108. https://doi.org/10.1093/treephys/24.10.1099 PMID: 15294756

68. Scholz FG, Bucci SJ, Goldstein G, Meinzer FC, Franco AC, Miralles-Wilhelm F; Removal of nutrient limitations by long-term fertilization decreases nocturnal water loss in savanna trees. [Internet]. 2007. https://www.treesearch.fs.fed.us/pubs/29697

69. Wildt J, Kley D, Rockel A, Rockel P, Segschneider HJ. Emission of NO from several higher plant species. J Geophys Res Atmospheres. 1997; 102: 5919–5927. https://doi.org/10.1029/96JD02968

70. García-Mata C, Lamattina L. Nitric Oxide Induces Stomatal Closure and Enhances the Adaptive Plant Responses against Drought Stress. Plant Physiol. 2001; 126: 1196–1204. https://doi.org/10.1104/pp.126.3.1196 PMID: 11457969

71. Feng Y-L, Auge H, Ebeling SK. Invasive Buddleja davidii allocates more nitrogen to its photosynthetic machinery than five native woody species. Oecologia. 2007; 153: 501–510. https://doi.org/10.1007/s00442-007-0759-2 PMID: 17534664

72. Hikosaka K, Hirose T. Nitrogen uptake and use by competing individuals in a Xanthium canadense stand. Oecologia. 2001; 126: 174–181. https://doi.org/10.1007/s004420000517 PMID: 28547615

73. Aranda I, Pardo F, Gil L, Pardos JA. Anatomical basis of the change in leaf mass per area and nitrogen investment with relative irradiance within the canopy of eight temperate tree species. Acta Oecologica. 2004; 25: 187–195. https://doi.org/10.1016/j.actao.2004.01.003

74. de la Riva EG, Olmo M, Poorter H, Ubera JL, Villar R. Leaf Mass per Area (LMA) and Its Relationship with Leaf Structure and Anatomy in 34 Mediterranean Woody Species along a Water Availability Gradient. PLOS ONE. 2016; 11: e0148788. https://doi.org/10.1371/journal.pone.0148788 PMID: 26867213

75. Edwards EJ, Chatelet DS, Sack L, Donoghue MJ. Leaf life span and the leaf economic spectrum in the context of whole plant architecture. J Ecol. 2014; 102: 328–336. https://doi.org/10.1111/1365-2745.12209

76. Bussotti F, Pollastrini M, Cascio C, Desotgiu R, Gerosa G, Marzuoli R, et al. Conclusive remarks. Reliability and comparability of chlorophyll fluorescence data from several field teams. Environ Exp Bot. 2011; 73: 116–119. https://doi.org/10.1016/j.envexpbot.2010.10.023

77. Mittler R. Oxidative stress, antioxidants and stress tolerance. Trends Plant Sci. 2002; 7: 405–410. https://doi.org/10.1016/S1360-1385(02)02312-9 PMID: 12234732

78. Bassin S, Volk M, Fuhrer J. Species Composition of Subalpine Grassland is Sensitive to Nitrogen Deposition, but Not to Ozone, After Seven Years of Treatment. Ecosystems. 2013; 16: 1105–1117. https://doi.org/10.1007/s10021-013-9670-3

79. Palmroth S, Bach LH, Nordin A, Palmqvist K. Nitrogen-addition effects on leaf traits and photosynthetic carbon gain of boreal forest understory shrubs. Oecologia. 2014; 175: 457–470. https://doi.org/10.1007/s00442-014-2923-9 PMID: 24705693

80. Yao X, Liu Q. Changes in morphological, photosynthetic and physiological responses of Mono Maple seedlings to enhanced UV-B and to nitrogen addition. Plant Growth Regul. 2006; 50: 165. https://doi.org/10.1007/s10725-006-9116-4

81. Velikova V, Fares S, Loreto F. Isoprene and nitric oxide reduce damages in leaves exposed to oxidative stress. Plant Cell Environ. 2008; 31: 1882–1894. https://doi.org/10.1111/j.1365-3040.2008.01893.x PMID: 18811730

82. Neill SJ, Desikan R, Hancock JT. Nitric oxide signalling in plants. New Phytol. 2003; 159: 11–35. https://doi.org/10.1046/j.1469-8137.2003.00804.x

83. Beligni MV, Lamattina L. Nitric oxide counteracts cytotoxic processes mediated by reactive oxygen species in plant tissues. Planta. 1999; 208: 337–344. https://doi.org/10.1007/s004250050567

84. Fares S, Loreto F, Kleist E, Wildt J. Stomatal uptake and stomatal deposition of ozone in isoprene and monoterpene emitting plants. Plant Biol. 2008; 10: 44–54. https://doi.org/10.1055/s-2007-965257 PMID: 17538866

85. Loreto F, Pinelli P, Manes F, Kollist H. Impact of ozone on monoterpene emissions and evidence for an isoprene-like antioxidant action of monoterpenes emitted by Quercus ilex leaves. Tree Physiol. 2004; 24: 361–367. https://doi.org/10.1093/treephys/24.4.361 PMID: 14757575